

Large-Scale Characteristics of Wideband MIMO Channel in Rural Macro Environments

Wonsop Kim¹, Hyuckjae Lee

College of Information Science & Technology
Korea Advanced Institute of Science and Technology
Daejeon, Korea
{topsop¹, hjlee314}@kaist.ac.kr

Jae Joon Park, Myung-Don Kim, Hyun Kyu Chung

Mobile Telecommunication Research Division
Electronics and Telecommunications Research Institute
Daejeon, Korea
{jjpark, mdkim, hkchung}@etri.re.kr

Abstract— Based on the experimental results obtained from the extensive wideband MIMO channel measurements at 2.38, 3.705 and 5.25GHz in Line-Of-Sight (LOS) rural macro environments, the empirical Path Loss (PL) model is proposed for the IMT-Advanced systems. PL exponent, intercept, frequency dependent factor and standard deviation of Shadow Fading (SF) are obtained by using the Least Square (LS) method. It is found that the frequency dependent factor well reflects the measured PL at each carrier frequency. We investigate the frequency dependence of SF. It is found that the statistics of SF component are not dependent on frequency.

Keywords- least square, path loss, shadow fading.

I. INTRODUCTION

Beyond 3rd generation (B3G) was named officially IMT-Advanced by the International Telecommunication Union-Radiocommunications (ITU-R). For the IMT-Advanced system, the carrier frequency and bandwidth will be up to 3.6GHz and 100MHz, respectively. Since performance of MIMO system depends on the behavior of MIMO channel, efficient system for MIMO communication requires accurate knowledge of channel characteristics. Since the channel measurements and modeling works are most effective ways to get practical and accurate channel parameters and models at the frequency bands for IMT-Advanced system, the ITU-R Working Party 5D (WP5D) defines a channel model for IMT-Advanced system. Because the channel measurements were performed mainly in Europe [4] and [5], to contribute to IMT-Advanced channel model we conducted wideband MIMO channel measurements using wideband MIMO channel sounder, Band Exploration and Channel Sounding (BECS) 2006 Plus, at 2.38, 3.705 and 5.25GHz. In this measurement, the bandwidths at 2.38, 3.705 and 5.25 GHz are set to 20, 100 and 100 MHz respectively.

In this paper, the empirical PL model including PL exponent, intercept and frequency dependent factor for rural macro environment is developed based on measurement data at three different carrier frequencies, which can be used for system and cell design. It is found that the frequency dependent factor well reflects the measured PL at each carrier frequency. Information on the behavior of the SF component which is regarded as log normally distributed is also important for the system performance. We investigate the suitability of the log normal SF and determine whether the SF parameters are

dependent on carrier frequency or not. It is observed that the statistics of SF component are not dependent on frequency.

The paper is organized as follows. In the section II, the channel sounder architecture is described. Section III gives a brief description of the measurement campaign. Section IV presents the large scale characteristics. Finally, conclusions are given in Section V.

II. CHANNEL SOUNDER ARCHITECTURE

The architecture of BECS 2006 Plus system is shown in Fig. 1. The transmitter or receiver of BECS 2006 Plus can use maximum eight antenna elements. The system process at the transmitter is as follows. At the Baseband Unit (BBU), After the Pseudo Noise (PN) sequences go through a pulse shaping Root Raised Cosine (RRC) filter, the PN signals are downloaded to a signal generator. The output of a signal generator, the BPSK modulated signals, is fed into a high-speed digital-to-analog converter (DAC). At the RF Up/Down Converter Unit (TRXU), the IF signals are changed to RF signals. At the High Power Amplifier (HPA) and RF Switch and front-end Unit (RFFU), RF signals are amplified and radiated sequentially. The system process at the receiver is as follows. By the use of RFFU, data acquisition is sequentially performed in turn through all the antenna elements. At the TRXU, the RF signals are changed to IF signals. The down converted signals are fed to high-speed analog-to-digital converter (ADC) and Demodulated I-Q data is saved at the BBU. The external laptop computer stores the data for later analysis. The Timing Unit (TIMU) gives timing pulses for BBU, TRXU and RFFU. Table I shows the BECS 2006 Plus requirements.

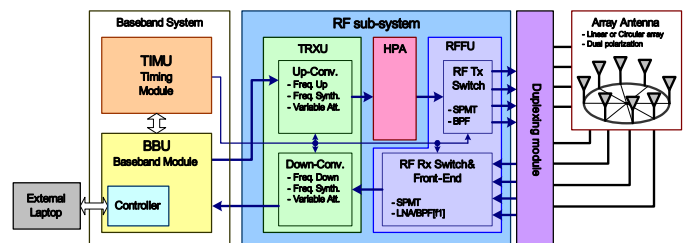


Figure 1. System architecture of BECS 2006 Plus

TABLE I. BECS 2006 PLUS REQUIREMENT

Parameter	Value		
	2.38GHz	3.705GHz	5.25GHz
Frequency	2.38GHz	3.705GHz	5.25GHz
Bandwidth [MHz]	20/10/5	100/40/20/10/5	100/40/20/10/5
PN Length [chips]	31 ~ 4095		
Number of Tx Antennas	8		
Number of Rx Antennas	8		

TABLE II. MEASUREMENT CONFIGURATION

	2.38GHz	3.705GHz	5.25GHz
Bandwidth [MHz]	20	100	100
Number of Antennas	Tx (ULA): 4 Rx (ULA): 4	Tx (ULA): 4 Rx (ULA): 4	Tx (ULA): 4 Rx (ULA): 4
Tx antenna height [m]	27	27	20
Rx antenna height [m]	2	2	2
Tx antenna spacing [λ]	10	10	10
Rx antenna spacing [λ]	0.5/2.0	0.5/2.0	0.5/2.0



Figure 2. Measurement environments

III. MEASUREMENT CAMPAIGN

Fig. 2 shows the measurement environments. The measurement campaign was conducted in LOS rural macro environment in Jeju, Korea using the BECS 2006 Plus system. The transmit (Tx) system uses a Uniform Linear Array (ULA) consisting of four antennas, which are collinear dipole arrays respectively. The receive (Rx) system uses ULA consisting of four antennas, which are quarter wave monopoles respectively. The Tx antenna array is located on the rooftop of a building and marked on the center of the Fig. 2 with Tx. The Rx antenna array is mounted on the roof of a car. From the starting point of each route, R_1, R_2, R_3 and R_4, we drive along each route at a speed of around 10 km/h. For a route at each carrier frequency, we perform two cases of measurements where Tx antenna spacing is fixed to 10λ and Rx antenna spacing is used to 0.5λ or 2.0λ . λ denotes the wavelength. The measurement configurations at 2.38, 3.705 and 5.25GHz are summarized in Table II.

IV. LARGE SCALE CHARACTERISTICS

The total received power at Tx-Rx distance d is given by

$$P_r(d) = P_D(d) + P_S(d) + P_F(d) \quad (1)$$

where P_D is the component of received power proportional to PL exponent n , $P_S(d)$ is the slow fading component and occurs mainly due to the effects of buildings and terrain features, $P_F(d)$ is the fast fading component and occurs mainly due to multipath effects. All values are in dB scale. The slow fading is also referred to SF.

A. Path Loss Model

The PL is defined as

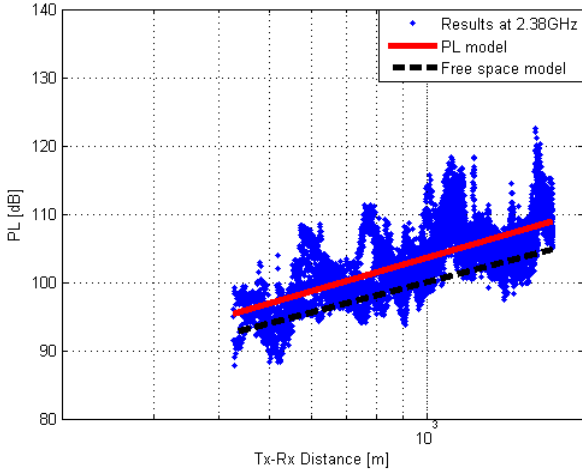
$$PL = P_T - P_R + G_T + G_R \quad (2)$$

where P_T , P_R , G_T and G_R are TX and Rx powers, Tx and Rx antenna gains respectively. All values are in dB scale. In this measurements Tx antenna gains for 2.38, 3.705 and 5.25GHz are 11, 12 and 9.2 dBi respectively and Rx antenna gains for 2.38, 3.705 and 5.25GHz are 0, 1 and 2 dBi respectively. The free-space PL is given by Friis free-space equation [1] as

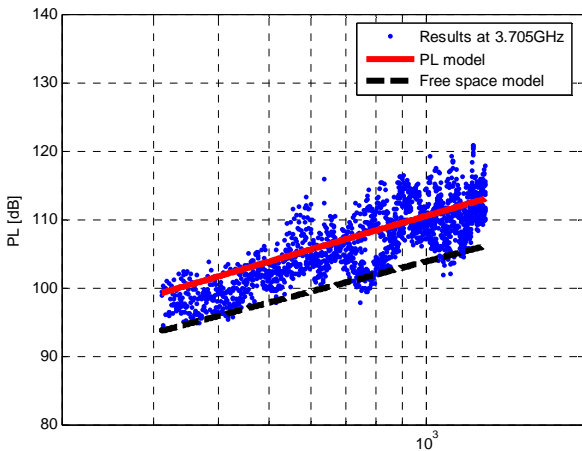
$$\begin{aligned} PL_{FS} &= 20 \log_{10} \left(\frac{4\pi d}{\lambda} \right) \\ &= 20 \log_{10}(d) + 32.4 + 20 \log_{10}(f_c) \end{aligned} \quad (3)$$

where Tx and Rx antenna gains are excluded, d is the Tx-Rx distance in meter and f_c is the carrier frequency in GHz. Using the LS method, we fit the measured PL values to the following PL model

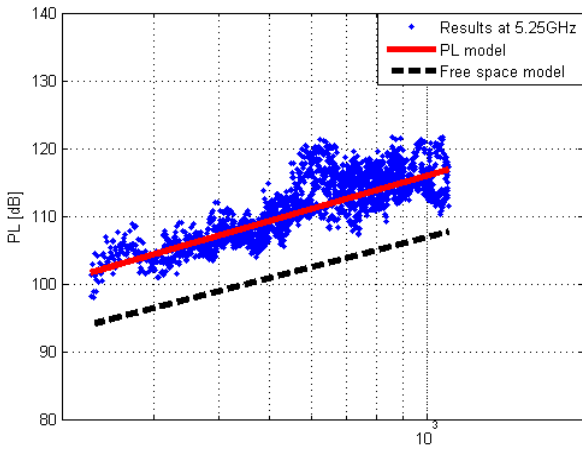
$$PL = 10n \log_{10}(d) + B + C \log_{10}(f_c) \quad (4)$$



(a) Results at 2.38GHz



(b) Results at 3.705GHz



(c) Results at 5.25GHz

Figure 3. Path loss results at 2.38, 3.705 and 5.25GHz

where n is the PL exponent, B is the intercept and C describes the frequency dependent factor. Fig. 3 shows the PL model fit expressed by (4) with the PL exponent $n = 2.22$.

$$PL = 22.2 \log_{10}(d) + 23.4 + 36 \log_{10}(f_c) \quad (5)$$

It is found that the frequency dependent factor $C = 36$ well reflects the measured PL at each carrier frequency. In this measurement, the Tx-Rx distance is up to about 1800 m, which is not long enough to define the breakpoint [2] for the more severe PL at longer distance. Therefore, the valid Tx-Rx distance range for the PL model is approximately from 200 to 1800 m.

B. Shadow fading characteristics

In order to estimate SF component $P_S(d)$, we first separate $P_R(d)$ into large scale part, $P_D(d) + P_S(d)$, and small scale part, $P_F(d)$. The $P_F(d)$ can be properly removed by averaging $P_R(d)$ with 40λ window size [3] at each carrier frequency. $P_D(d)$ can be calculated from (5). Then $P_S(d)$ is obtained by removing $P_D(d)$ from the large scale part of the total received power. Fig. 4 shows that a log-normal distribution provides a good match to the empirical probability density function (pdf) of the SF component which include the data at 2.38, 3.705 and 5.25GHz. From Fig. 5, it is not expected that the statistics of SF would be frequency dependent. We believe this is because the SF fluctuation is actually a result of the birth and death of multipaths, which correspond to the changing scatterers along Rx movement. Table III shows the average standard deviation of SF.

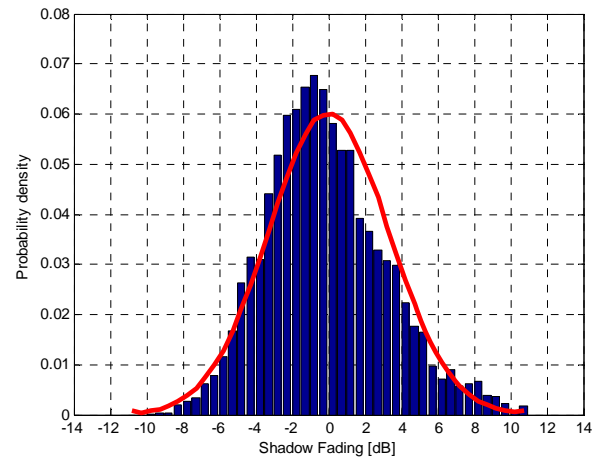


Figure 4. Shadow fading with log normal distribution

TABLE III. AVERAGE STANDARD DEVIATION σ OF SF

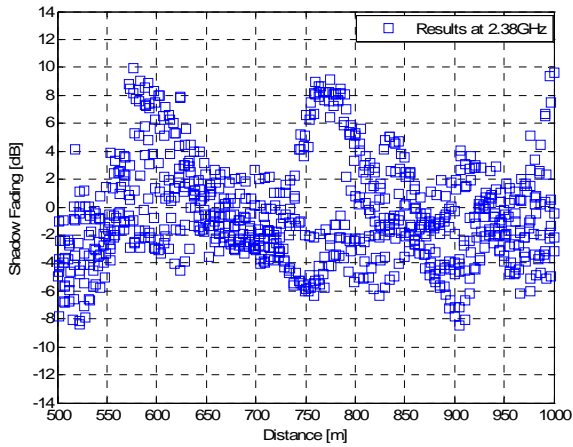
Scenario	σ at 2.38GHz [dB]	σ at 3.705GHz [dB]	σ at 5.25GHz [dB]
LOS	3.67	2.89	2.59

V. CONCLUSIONS

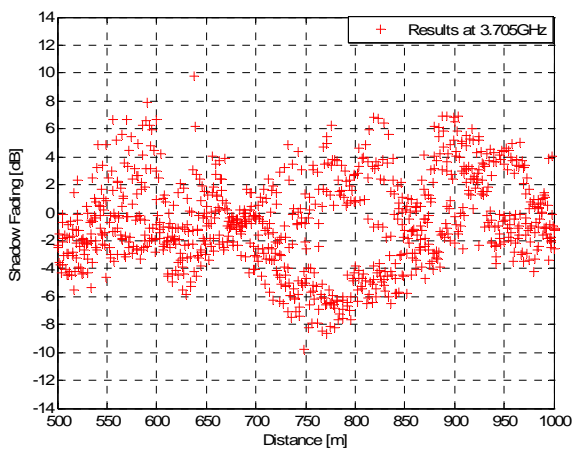
This paper has presented measurement results of wideband MIMO channel using the BECS 2006 Plus in LOS rural macro environments. The propagation characteristics at 2.38, 3.705 and 5.25GHz have been provided based on an analysis of measurement data. The empirical log-distance PL model is proposed with exponent of 2.22 and frequency dependent factor of 36. It is found that the frequency dependent factor well reflects the measured PL at each carrier frequency. It is observed that the statistics of SF component is not dependent on frequency. The results should be useful for designing communication systems and for simulating large-scale effects on systems in the laboratory.

REFERENCES

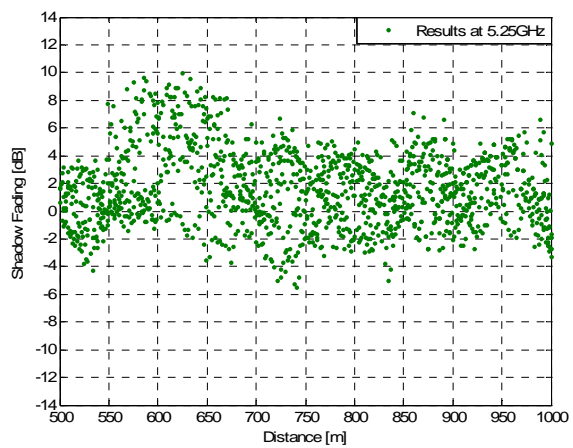
- [1] T. S. Rappaport, *Wireless Communications: Principles Practice*. Upper Saddle River, NJ: Prentice-Hall, 1996.
- [2] Sub-Working Group Evaluation, "Guidelines for evaluation of radio interface technologies for IMT-Advanced," Document 5D/TEMP/99-E, 14 October 2008.
- [3] W. C. Y. Lee, "Estimate of local average power of a mobile radio signal," *IEEE Trans. Veh. Technol.*, vol. 34, pp. 22-27, Feb. 1985.
- [4] A. Algans, K. I. Pedersen, P. E. Mogensen, "Experimental Analysis of the Joint Statistical Properties of Azimuth Spread, Delay Spread, and Shadow Fading," *IEEE J. Select. Areas Commun.*, vol. 20, no. 3, pp. 523-531, April 2002.
- [5] X. Zhao, J. Kivinen, Pertti Vainikainen, and K. Skog, "Propagation Characteristics for Wideband Outdoor Mobile Communications at 5.3 GHz," *IEEE J. Select. Areas Commun.*, vol. 20, no. 3, pp. 507-514, April 2002.



(a) Results at 2.38GHz (use the data of 8 measurements from 4 routes)



(b) Results at 3.705GHz (use the data of 8 measurements from 4 routes)



(c) Results at 5.25GHz (use the data of 8 measurements from 4 routes)

Figure 5. Shadow fading results at 2.38, 3.705 and 5.25GHz